Acoustical source characterization by using recursive Wiener filtering

Mingsian R. Bai
Department of Mechanical Engineering, National Chiao-Tung University, 1001 Ta-Hsueh Road, Hsin-Chu 30050, Taiwan, Republic of China

(Received 17 December 1993; accepted for publication 11 January 1995)

This paper discusses a feedback iteration technique that provides the enhancement of backward reconstruction in acoustical imaging. Reconstruction of a vibrating surface motion from acoustic holographic data causes computational difficulties because the problem is ill posed. In order to deal with these difficulties, a method is developed based on a recursive algorithm, where the inverse problem is converted to a well-posed forward propagation problem. An initial guess regarding the source images is required to activate the iterative inversion method. Then, the tentative image is propagated forward to the hologram plane and the residue is determined. Next, a feedback operator is used to process the residue by which the image is updated. Two types of feedback operators were investigated: (1) a Wiener suboptimal operator, and (2) a dynamic, optimal operator (designed subject to minimum mean-square-error optimization criteria). The performance of these iteration methods was investigated by numerical simulations of the holographic reconstruction of a baffled piston field. Both iteration methods provided satisfactory convergence and were found to be relatively insensitive to the choice of initial guess and noise parameters used in the feedback operators.

PACS numbers: 43.20.Ks, 43.20.Ye

INTRODUCTION

An increasing interest has been seen in recent years in the study of acoustical imaging which has become an important tool of analysis in acoustic research.[1] Among the applications of acoustical imaging, backward reconstruction exhibits advantages over other methods for source radiation analysis. For instance, backward reconstruction can be used for noise source identification. This approach is more effective in dealing with distributed sources than some other *point-to-point* methods (e.g., multiple input-one output spectral analysis that provides the estimate of a *lumped* contribution from each source at certain known location.[2]

The main idea of backward reconstruction is to back-propagate the field to the source surface on the basis of the field measured on a surface in the vicinity of the source. Given the properties of the medium and the geometry of the source boundary, we are seeking to determine the acoustic field or radiation impedance on the source surface. In this connection, the problems relevant to this paper are different from the inverse problems in general where the actual physical boundaries of the sources are not known. Backward reconstruction *per se* is an inverse problem in a somewhat restricted sense since some prior knowledge is required. For the backward reconstruction considered in the study, it is well known that this type of problem suffers from numerical discontinuity despite that the existence and uniqueness of their solutions are fulfilled in the mathematical sense.[3–6] More precisely, associated with the process of backward reconstruction, the measured data reveals very little information about the source and its near-field. Two dramatically different sources are likely to be mapped into the far-field image within the same level of tolerance.

In order to alleviate this numerical difficulty, a variety of methods have been invented. The majority of these schemes fall into the class of windowing usually performed in the wave spectrum domain, e.g., Bartlett, Blackman, Hamming, Hanning, Kaiser, exponential, Butterworth, and Wiener filtering.[7–9] Alternatively, backward reconstruction can be carried out in the spatial domain through certain pseudoinversion procedure, e.g., singular value decomposition.[8] Most of these methods achieve numerical stability by means of the attenuation of the high-frequency components corresponding to small eigenvalues in the reconstructed image. A more thorough survey can be found in Ref. 10.

In contrast to the above-mentioned methods, the objective of this paper is to propose a feedback iteration technique that provides the improvement of backward reconstruction in acoustical imaging. In the development of this method, prior knowledge about the source such as global bounds, smoothness conditions, statistical properties, and geometric extent is incorporated in the computational algorithms as the supplementary constraints in order to restrict the class of admissible functions. Consequently, the numerical anomalies are considerably reduced through the restoration of the solution continuity. To this end, the proposed method employs an iterative deconvolution concept[11,12] that reformulates the problem is such a way that the ill-posed backward reconstruction is converted to the well-posed forward propagation. In diffraction tomography, two similar methods have been used in the past.[13–15] These techniques employ iterative algorithms for wave tomography that are generalizations of the ART and SIRT algorithms of x-ray tomography.

This method proposed in this paper requires an initial guess of source image in order to activate the iteration process. Then, this tentative image is forward propagated to the

 0001-4966/95/97(5)/2657/7/$6.00

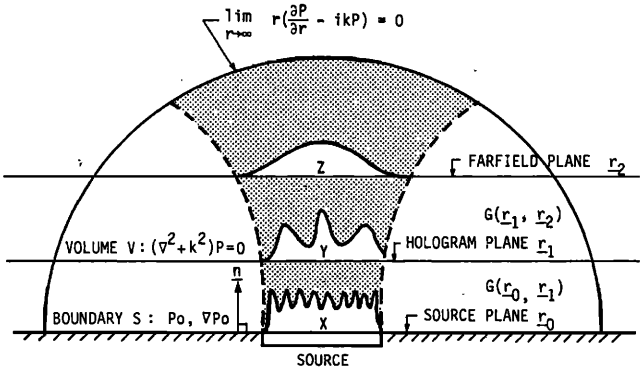

FIG. 1. Boundary-value problem in acoustical imaging.

hologram plane, and the residue is determined. Next, a feedback operator is applied to process the residue by which the image is updated. The effectiveness of this method relies largely upon the choice of the feedback operator. In this study, we have developed two types of feedback operators: (1) A Wiener-type or nonoptimal operator, and (2) a dynamic-type or optimal operator. In addition, this method is further enhanced when the constraint function based on prior knowledge about the source, e.g., geometric extent, is incorporated.

Numerical simulations were conducted to compare the iteration techniques with conventional direct inversion methods. In the simulation, various iterative inversion methods developed in this study were applied to the reconstruction of the near-field of a vibrating piston of finite size in a rigid baffle. Results of these simulations show the potential for improvement of the backward reconstruction of acoustical imaging with the use of the iterative inversion technique.

I. THEORY

A. Inverse problem in acoustics

The inverse problem in acoustics is schematically shown in Fig. 1. A planar acoustic source embedded in a rigid piston radiates energy away from its surface. Assume that only monochromatic fields are of concern and the sound-pressure samples can be measured only in the vicinity instead of directly on the surface of the source. The objective is to calculate the sound-pressure samples on the source surface, called here the image plane. This calculation is based upon the sound pressure measured on the hologram plane. In this case, spatial transformation between two planes separated by a source-free region can be expressed with a Fredholm integral equation of the first kind

$$p(x,y,z)=\int_S G_D(x-x_0,y-y_0,z-z_0)p(x_0,y_0,z_0)ds, \tag{1}$$

where $p(x,y,z)$ and $p(x_0,y_0,z_0)$ are the pressure on the hologram plane and source plane S, respectively,

$$p(x_0,y_0,z_0)\in S,\quad G_D=(z/2\pi)(1-ikr)\exp(ikr)/r^3$$

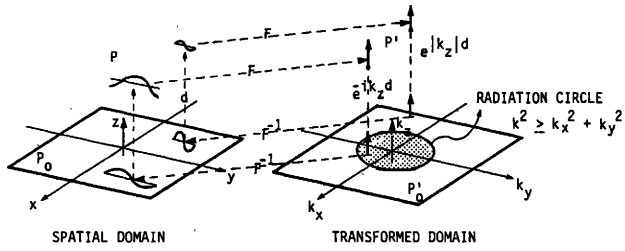

FIG. 2. Illustration of the holographic imaging and ill posed nature of the inverse problem (after Ref. 1).

is the transfer function of the planar half-space Dirichlet problem, $r=[(x-x_0)^2+(y+y_0)^2+(z-z_0)^2]^{1/2}$, and k is the wave number. The source field $p(x_0,y_0,z_0)$ can be solved by performing the deconvolution of Eq. (1) via the two-dimensional Fourier transform.

$$p'(k_x,k_y,z_0)=\begin{cases} p'(k_x,k_y,z_0)e^{-id(k^2-k_x^2-k_y^2)^{1/2}}, & k^2\geq k_x^2+k_y^2, \\ p'(k_x,k_y,z_0)e^{d(k_x^2+k_y^2-k^2)^{1/2}}, & k^2<k_x^2+k_y^2, \end{cases} \tag{2}$$

where $d=z-z_0\geq 0$ is the distance of transformation and $p'(k_x,k_y,z_0)$ is the two-dimensional Fourier transform of $p(x,y,z)$ with respect to the Cartesian coordinates x and y. Hence, the deconvolution basically reverses the phase shift without altering the magnitude for the propagation components inside the radiation circle ($k^2\geq k_x^2+k_y^2$). On the other hand, for the evanescent components outside the radiation circle ($k^2<k_x^2+k_y^2$), the deconvolution restores the exponentially decayed magnitude without changing the phase and in effect amplifies the measurement, modeling, and processing errors that eventually smear the image results (see Fig. 2). Thus some filtering is required to reduce the distortions; however, at the same time, high-frequency components that contain a certain amount of real information are lost (see Fig. 3).

In summary, numerical solutions of the acoustic inverse problem are generally nonunique and unstable. This is because convolution represents a smoothing process that causes the near-field details to become obscured as the field propagates away from the source. Conversely, in backward reconstruction, the input may be exceedingly sensitive to small changes in the output. Small errors in the output are magnified and eventually the accuracy becomes very poor.

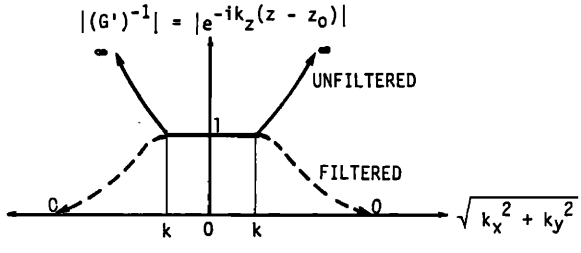

FIG. 3. Filtering of evanescent waves in the transformed domain.

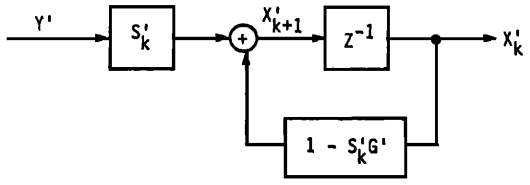

FIG. 4. Control analogy for the iterative inversion concept.

B. Iterative inversion techniques for acoustical imaging

1. Basic formulation of the nonoptimized algorithm

An iteration method is developed such that the ill-posed nature of the backward reconstruction can be alleviated by converting the inverse problem into a forward one. Referring to Fig. 1, the field transformation in Eq. (1) can be written more succinctly in the form of convolution:

$$G*X=Y, \tag{3}$$

where $X=p(x_0,y_0,z_0)$ is source field to be reconstructed, $Y=p(x,y,z)$ is the sound field measured on the hologram plane, and $G=G_D(x-x_0,y-y_0,z-z_0)$ is the transfer function relating the fields X and Y. The idea proposed in this paper of getting the source field X is to, instead of doing the deconvolution of Eq. (3) directly, recursively modify X such that the error between the propagated and the measured image fields of Y is negligibly small. That is, in the iteration k, the trial source filed X_k is updated on the basis of the residual field $R_k=Y-G*X_k$ through the introduction of a feedback operator S_k:

$$X_{k+1}=X_k+S_k*R_k. \tag{4}$$

In doing so, the ill posedness can be alleviated since the inverse problem has been converted into a forward one. Here, a control analogy for this iterative concept can be drawn as in Fig. 4. The task involved can be defined as to properly adjust the feedback operator S_k such that numerical stability and convergence of backward reconstruction is improved.

The terms of convergence need to be commented. Assume that the feedback operator is constant for each iteration, say $S_k=S$. By performing the 2-D Fourier transformation on the iteration formula, it can be verified that the necessary and sufficient condition for convergence is

$$|1-S'G'|<1, \tag{5}$$

where $||$ denotes the complex norm and prime ($'$) denotes each transformed quantity in the (k_x,k_y,z) domain. In addition, when the condition of Eq. (5) is satisfied, the iteration method in the limit is equivalent to the direct inverse filter, i.e.,

$$\lim_{k\to\infty} X'_k=G'^{-1}Y'. \tag{6}$$

It should be noted that Eq. (6) does not imply that direct inverse filtering is superior to the iteration method because G'^{-1} is in general ill posed and difficult to implement in numerical computations.

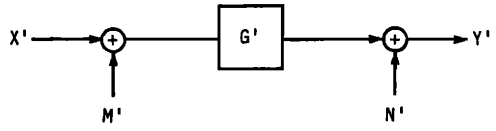

FIG. 5. Block diagram of a general system.

The next step in our development is to choose the feedback operator that satisfies the condition of convergence stated in Eq. (5). The Wiener filter was chosen for its simplicity:[8]

$$S'=(G')^{-1}[1+\alpha_1(\beta+|G'|^{-2})], \tag{7}$$

where $\alpha_1\geq 0$ and $\beta\geq 0$ are constant parameters. Note that the evanescent components will result in slower convergence.

2. Optimized algorithm and the constraint function

Up to this point, no special condition has been imposed on the choice of the feedback operator except that convergence is guaranteed. However, we can improve the convergence by taking into account some optimization criteria, which is the crux of the following proposed technique.

Referring to a general system shown in Fig. 5, the governing equation (in the transformed domain) takes the form:

$$Y'=G'(X'+M')+N', \tag{8}$$

where X' is the input, Y' is the output, G' is the transfer function, and M',N' are the statistically uncorrelated noise at the input and output, respectively. By writing the residual term explicitly, the recursive formulas of Eq. (4) can be expressed as

$$X'_k=X'_{k-1}+S'_{k-1}(Y'-G'X'_{k-1}). \tag{9}$$

Combining Eqs. (8) and (9) yields

$$X'_k=X'_{k-1}+S'_{k-1}[G'(X'+M')+N'-G'X'_{k-1}]. \tag{10}$$

Next, we define the error in the source field X' during the kth iteration as

$$e_k=X'-X'_k. \tag{11}$$

Hence, the optimal feedback operator for the iterative reconstruction process can be obtained by minimizing the following square error in the calculated image X':

$$V_{x,k}=\langle e_k e_k^* \rangle, \tag{12}$$

where "$\langle\ \rangle$" denotes mean value. From Eqs. (10)–(12), this mean-square error can be written explicitly as

$$V_{x,k}=V_{x,k-1}(1-S'_{k-1}G')(1-S'_{k-1}{}^*G'^*) +S'_{k-1}S'_{k-1}{}^*[G'G'^*\langle M'M'^*\rangle+\langle N'N'^*\rangle], \tag{13}$$

where $\langle M'M'^*\rangle$ and $\langle N'N'^*\rangle$ are the mean-square input and output noise, respectively. With some algebraic manipulations, the optimal feedback operator is found to be

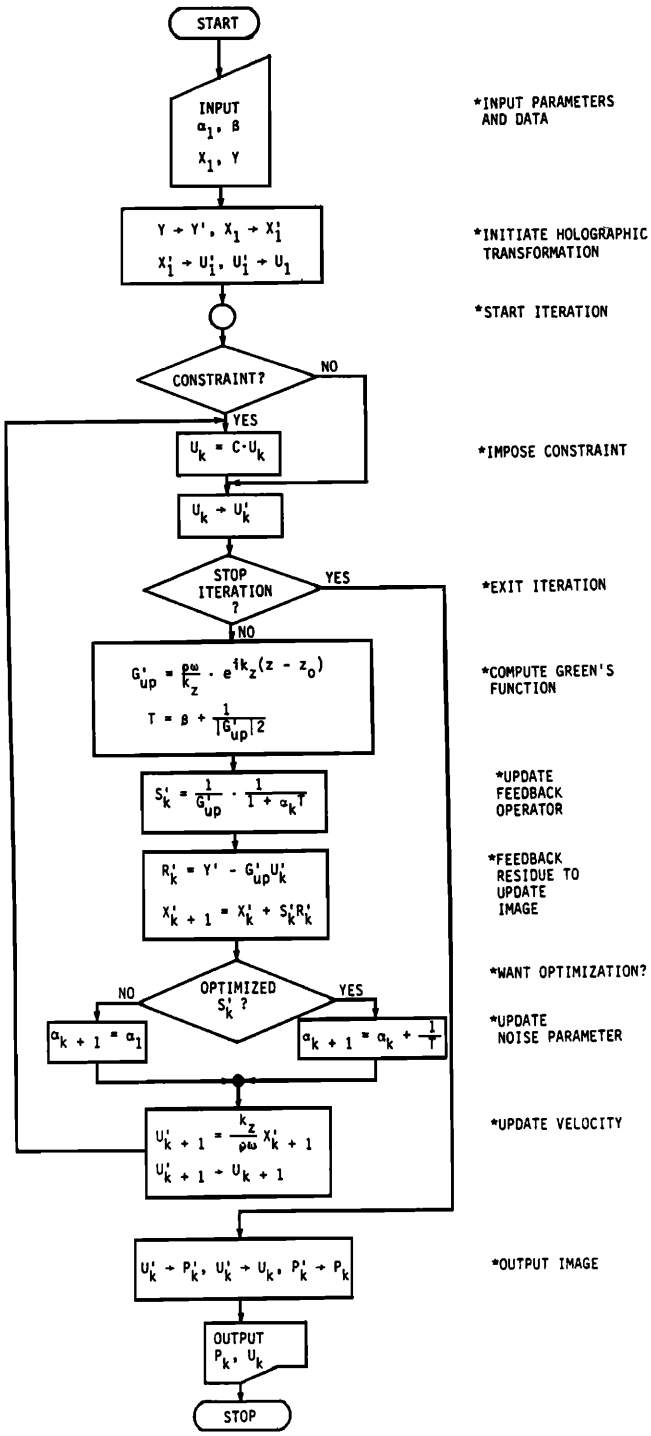

FIG. 6. Iterative inversion method-flow chart.

$$S_k' = G'^* V_{x,k} [G' G'^* (V_{x,k} + \langle M' M'^* \rangle) + \langle N' N'^* \rangle]^{-1}. \tag{14}$$

However, the following parameters must be introduced because the extraneous noise terms M' and N' are generally unknown *a priori:*

$$\alpha_k = \langle N' N'^* \rangle / V_{x,k}, \tag{15}$$

$$\beta = \langle M' M'^* \rangle / \langle N' N'^* \rangle, \tag{16}$$

$$T = \beta + |G'|^{-2}. \tag{17}$$

As a result, the iteration formulas can be simplified into

$$S_k' = [G'(1 + \alpha_k T)]^{-1}, \tag{18}$$

$$\alpha_{k+1} = \alpha_k + T^{-1}, \tag{19}$$

$$X_{k+1}' = X_k' + S_k' (Y' - G' X_k'). \tag{20}$$

In addition, it can be proved that the following properties hold:

$$X_k' = A_k' X_{k-1}' + S_k' Y', \tag{21}$$

$$A'_k=\alpha_{k-1}T(1+\alpha_{k-1}T)]^{-1}<1, \quad \text{if } \langle N'N'^*\rangle\neq 0, \tag{22}$$

where A'_k can be interpreted as a convergence factor. On the other hand, the following limiting properties are also true:

$$\text{when } k\to\infty, \quad \text{then } \alpha_k\to\infty, \quad S'_k\to 0, \quad A'_k\to 1, \tag{23}$$

$$V_{x,k}\to 0, \quad X'_k\to X', \tag{24}$$

$$V_{y,k}\to|G'|^2\langle M'M'^*\rangle+\langle N'N'^*\rangle,$$
$$Y'_k\to Y'-(G'M'+N'), \tag{25}$$

where $V_{y,k}=\langle(Y'-G'X'_{k-1})(Y'-G'X'_{k-1})^*\rangle$ is the mean square root of Y'.

It can be observed that the convergence of the iterative reconstruction process is guaranteed as shown in Eq. (22). The feedback operator is updated in a decelerating fashion as shown in Eq. (23). The influence of the hologram field Y' and the change of the source field X'_k are both decreasing during iterations, according to Eqs. (21) and (23). As the iteration goes on, the source image X'_k will always converge to the optimal value X, as shown in Eq. (24), even when the input noise M' and output noise N' are present in the system. On the other hand, the iterated output image Y'_k will converge asymptotically to $Y'-(G'M'+N')$ as the residue R'_k monotonically decreases, according to Eq. (25).

Further refinement of the iterative inversion technique can be achieved by incorporating the prior knowledge of the source. For example, if a source is embedded in a rigid baffle, the particle velocity should vanish outside the surface of the source. The surface velocity, therefore, can be updated by imposing the constraint before each iteration. The overall algorithm can be schematically represented by the flow chart shown in Fig. 6. With the variations of the feedback operator and constraints, four types of iterative inversion techniques can be implement on the basis of the algorithm in Fig. 6: (1) Nonoptimized feedback operator without source aperture constraint, (2) optimized feedback operator without source aperture constraint, (3) nonoptimized feedback operator with source aperture constraint, and (4) optimized feedback operator with source aperture constraint.

II. COMPUTER SIMULATION

Numerical simulations were conducted to investigate the iterative inversion techniques. These methods were tested with the sound field generated by a baffled piston of 4 cm radius vibrating in the air with the uniform surface velocity 1 m/s at the frequencies of 2 and 10 kHz ($ka=1.82$ and 9.11, respectively). The acoustic pressure in the hologram plane located 5 cm above the piston is generated with the sampling of Cartesian coordinates (aperture $D=0.248$ m, number of point $N=32$, spacing $\Delta x=8$ mm). Five spatial transformation methods including direct Wiener filtering and the previously discussed four iterative inversion techniques were used to reconstruct the sound pressure on the source surface (the distance of transformation is therefore 5 cm). The hologram data was first processed by the direct Wiener filter with the noise parameter denoted by α_i. Then the results from the direct Wiener filter were used as the initial guess for the iteration methods (with the noise parameters denoted by α_1 and with the number of iterations denoted by $N_{it}=40$). The simulated cases consist of numerous combinations of α_i and α_1 (each with three different levels).

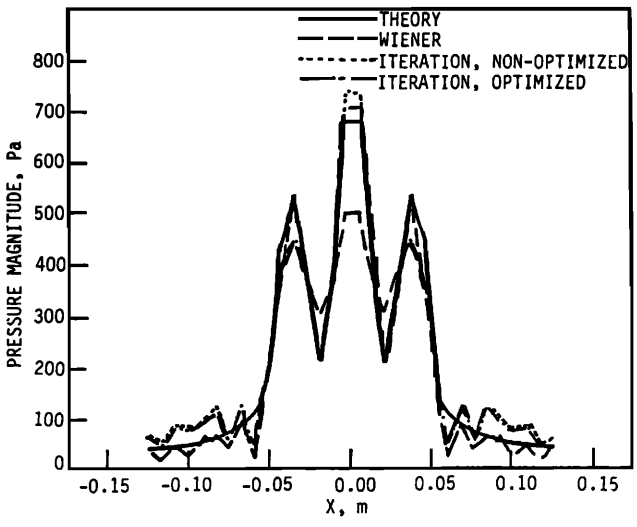

FIG. 7. Pressure magnitude on the surface of a baffled piston ($ka=9.1$) reconstructed from a hologram plane located 5 cm above a source with $\alpha_i=0.01$ and $\alpha_1=0.1$.

Because of limited space, only the representative cases are shown in Figs. 7–10. The comparison of Figs. 7 and 3 shows that the iterative inversion techniques are relatively insensitive to the choice of the noise parameter α_i in the initial guess and that they converge satisfactorily to the desired solutions. A slightly large noise parameter in the iteration methods is in general the preferable choice. As α_1 decreases, the iteration method based on an optimized feedback operator with the aperture constraint function provides more accurate results (see Fig. 9). The low-frequency case (2 kHz), where a relatively large amount of evanescent waves are present, is shown in Fig. 10. We observe that the iteration

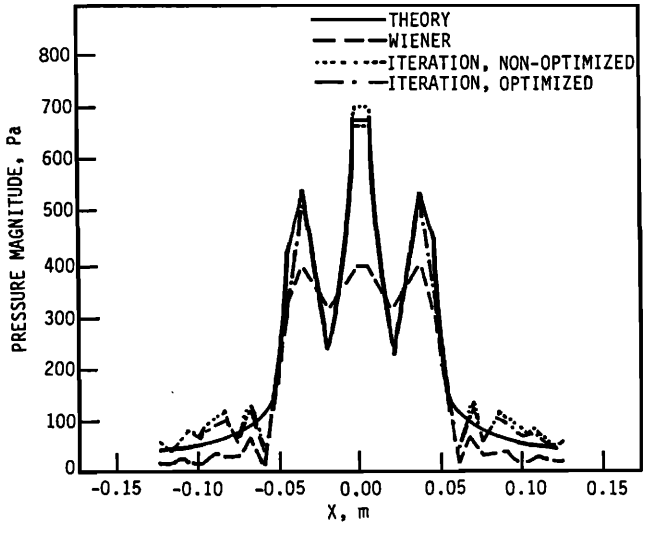

FIG. 8. Pressure magnitude on the surface of a baffled piston ($ka=9.1$) reconstructed from a hologram plane located 5 cm above a source with $\alpha_i=0.1$ and $\alpha_1=0.1$.

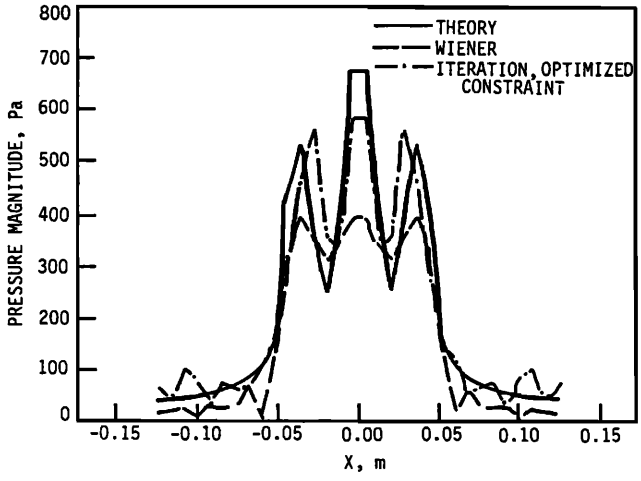

FIG. 9. Pressure magnitude on a surface of a baffled piston ($ka=9.1$) reconstructed from a hologram plane located 5 cm above a source with $\alpha_i=0.1$ and $\alpha_1=0.0025$.

method based on the optimized feedback operator provides better results than the one based on a nonoptimized operator, especially when the constraint was imposed. The better convergence of the optimized feedback operator over the nonoptimized operator can be attributed to the optimized operator being dynamically updated in a decelerating fashion according to the minimum mean-square-error criteria, while for the nonoptimized operator the noise parameter is kept constant during iterations.

Thus far we have been dealing with the ill-posed nature of the problem resulting from the errors involved in numerical simulations (modeling, sampling, discretization, finite aperture, etc.). In practical applications, the overall noise contains not only the numerical errors but also the experimental errors (extraneous noise, boundary interactions, measurement errors, etc.). Nevertheless, the iterative inversion methods can still provide significant improvement in the reconstructed image in comparison with the direct Wiener filtering method. This fact is illustrated in Fig. 11 where the hologram data is contaminated with synthetic Gaussian noise in order to simulate more realistic experimental signals. Therefore, the previous observations in Figs. 7–10 still apply even for the cases where physical noise is present.

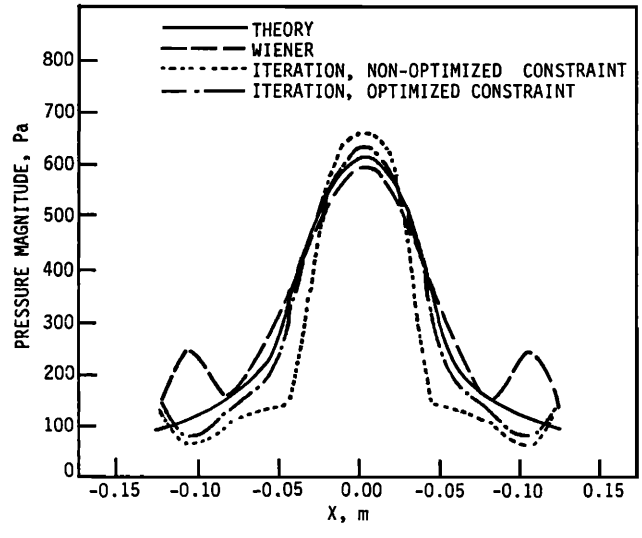

FIG. 10. Pressure magnitude on a surface of a baffled piston ($ka=1.8$) reconstructed from a hologram plane located 5 cm above a source with $\alpha_i=0.0025$ and $\alpha_1=0.01$.

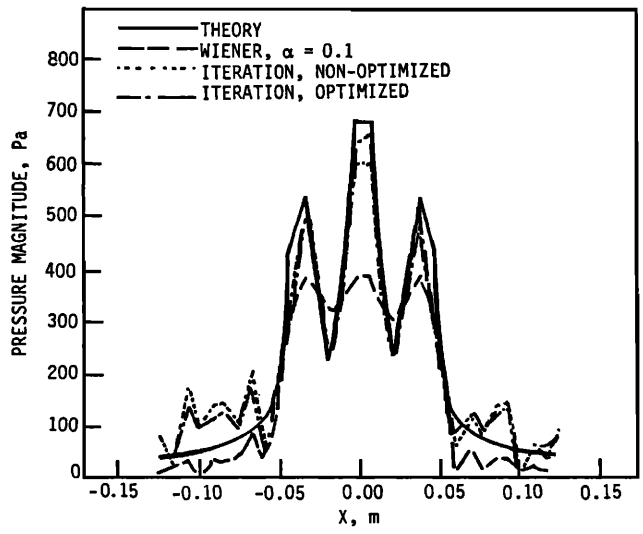

FIG. 11. Pressure magnitude on a surface of a baffled piston ($ka=9.1$) reconstructed from a hologram plane located 5 cm above a source with $\alpha_i=0.01$ and $\alpha_1=0.1$. Field is contaminated with a Gaussian noise.

III. CONCLUSION

It is evident from the numerical simulations that the iterative inversion techniques with all four types of feedback operators exhibit stable behavior and provide excellent reconstructed images. The iterative methods, though not as simple as the direct Wiener filtering (the computation time on Vax 11/785 is approximately 200 s for 40 iterations versus 30 s in a 32×32 case), can generally improve the source image with reasonable initial guess and noise parameters.

In some cases, the iterative inversion techniques are superior to the direct Wiener filtering; however, their performance depends largely upon the characteristics of the field of interest and the values of noise parameters. However, in those cases where it is difficult to find the optimal noise parameters for Wiener filtering, the more sophisticated iterative inversion methods can generally guide us to the desired solution with minimal efforts of trial and error.

Some guidelines in applying the iterative inversion techniques are in order. Despite the previously discussed low sensitivity of the iteration methods to the initial guess of the image, heavy filtering is required to avoid false convergence. With a reasonable initial guess, one can usually obtain a satisfactory image by choosing a somewhat large noise parameter within a sufficient number of iterations. For low-frequency sources, it is advisable to use the iteration method based on an optimized feedback operator with constraint. In some cases, however, the constraint might cause slow con-

vergence at the central region of the source, and thus the noise parameter α_1 must not be too large.

The iterative inversion technique appears to be a promising alternative to other techniques because of higher accuracy and flexibility in dealing with inverse reconstruction. However, the iteration method is not restricted to acoustic imaging, and it can be readily extended for more general inverse problems. In addition, the potential of iterative inversion techniques in industrial applications, e.g., source characterization (shape and motion) and noise source identification, will be explored by experimental investigations in the future.

ACKNOWLEDGMENT

The work was supported by the National Science Council in Taiwan, Republic of China, under project number NSC-81-0401-E009-571.

[1] D. Maynard, E. G. Williams, and Y. Lee, "Nearfield acoustic holography: I. Theory of generalized holography and the development of NAH," J. Acoust. Soc. Am. **78**, 1395–1413 (1985).

[2] S. Bendat and A. G. Piersol, *Engineering Applications of Correlation and Spectral Analysis* (Wiley–Interscience, New York, 1980).

[3] F. Santosa, *Inverse Problems of Acoustic and Elastic Waves* (SIAM, Philadelphia, 1984).

[4] P. Baltes, *Inverse Scattering Problems in Optics* (Springer-Verlag, New York, 1980).

[5] P. Baltes, *Inverse Source Problems in Optics* (Springer-Verlag, New York, 1978).

[6] K. Chadan and P. C. Sabatier, *Inverse Problems in Quantum Scattering Theory* (Springer-Verlag, New York, 1977).

[7] C. Gonzalez and P. Wintz, *Digital Image Processing* (Addison-Wesley, Reading, MA, 1979).

[8] K. Pratt, *Digital Image Processing* (Wiley, New York, 1978).

[9] G. S. Kino, *Acoustic Waves* (Prentice-Hall, New York, 1987).

[10] T. S. Huang, *Picture Processing and Digital Filtering* (Springer-Verlag, New York, 1979).

[11] E. Dudgeon and R. M. Mersereau, *Multidimensional Digital Signal Processing* (Prentice Hall, Englewood Cliffs, NJ, 1984).

[12] R. W. Schafer, "Constrained iterative restoration algorithms," Proc. IEEE **69**(4), 432–450 (1981).

[13] A. J. Devaney, "Reconstructive tomography with diffracting wavefields," Inverse Problems **2**, 161–170 (1986).

[14] K. Ladas and A. J. Devaney, "Generalized ART algorithm for diffraction tomography," Inverse Problems **7**, 109–121 (1992).

[15] K. Ladas and A. J. Devaney, "Iterative methods in geophysical diffraction tomography," Inverse Problems **8**, 119–132 (1992).